Mediterranean heat waves and wildfires of July-August 2021 in the southern part of Turkey

Zahide Acar (zacar@comu.edu.tr)
Çanakkale Onsekiz Mart University
Barbaros Gonencgil
Istanbul University
Onur Halis
Istanbul University

Research Article

Keywords: Wildfire, Mediterranean region, Turkey, Heatwave

Posted Date: July 5th, 2022

DOI: https://doi.org/10.21203/rs.3.rs-1777015/v1

Abstract

Extreme weather events are experienced more frequently across the earth due to the effects of climate change. The high frequency of extreme weather events increases vulnerability in sensitive areas. In the Mediterranean Basin, which is one of the most sensitive areas, many countries have experienced wildfires in recent years. Turkey is one of the countries where forest fires occur frequently in the Mediterranean basin. Although the causes of the fire vary over the years, the problems caused by forest fires draw attention every year. Since 1990, there have been many forest fires across the country and the most areal losses caused by the Fires occurred in 1994, 2000 and 2008. The largest forest fires after these dates occurred in the summer of 2021.

The area where Turkey is most sensitive to fire is the Mediterranean climate region. Most of the fires, especially in this area, occur in an unnatural way such as negligence-accident, unsolved and intentional. The control mechanism in the spatial expansion of fires mostly depends on atmospheric conditions. Within the scope of the study, it was aimed to draw attention to the atmospheric conditions during the period of wildfires in many parts of Turkey in the summer of 2021 for various reasons. According to the calculations, the air temperatures before the start of the fire in the provinces of Antalya and Muğla are above the long-term averages of the stations here. In addition, the effects of the heat wave were observed at many stations before the fire.

Introduction

2021 has been one of the years in which extreme temperatures were seen over the Mediterranean Basin (Kaynak). Turkey's Mediterranean coasts have also been affected by these extreme events, both due to the impact of global climate change and the characteristic features of the Mediterranean climate.

Atmospheric disasters and the effects of these disasters are increasing every year. Today, atmospheric-based disasters cause more loss of life and property in Turkey. For example, the number of disasters experienced in 2020 was 321 earthquakes, 177 floods, and flashfloods and 270 storms, hail, extreme winter conditions, etc. are caused by climate-related events (AFAD, 2021).

Atmospheric disasters are divided into two main groups meteorological and climatological disasters (Kaynak). Extreme temperatures constitute an important part of climatological disasters. However, an important form of climatological origin disasters is forest and wildfires. On the other hand, fires are a great risk for climate zones with high sensitivity, such as the Mediterranean climate.

A wildfire is an uncontrolled fire that occurs in rural or virgin land. It is a type of fire that includes different areas such as forest, scrub, bush, meadow, dwarf tree, and peat fire. It is a type of fire that affects large areas and is not easy to stop and can spread rapidly under atmospheric conditions. It is a type of fire that can easily break out under arid and semiarid climates and is mostly seen in Australia (Kaynak). However, there is a potential to be seen in other arid, semiarid areas of the earth. Compared to previous years, the south of Europe corresponds to the period after the 1970s, when wildfire frequency increased due to

climate change and extreme events (Fernandes et al., 2010; Pausas and Fernandez-Munoz, 2012; Kovats et al., 2014). Mega fires triggered by extreme weather events have caused record burning areas in some Mediterranean countries in recent years. Most of these fires (approximately 55%) were caused by deliberated actions by people (San-Miguel-Ayanz et al., 2013). Mega fire events pose great threats to rural areas and their surroundings. Many researchers have also stated that atmospheric conditions had an intentional fire effect on wildfire events in Portugal, Spain, Italy, and Greece in recent years across the Mediterranean basin (Ex: San-Miguel-Ayanz et al., 2013; Vilar et al., 2009; Tedim et al.,2022; Baccui et al., 2021). In addition, wildfires are an important threat to the forests of Turkey, as in many parts of the Mediterranean Basin. Wildfires, which intensify in the summer months, seriously damage forest ecosystems. According to the evaluations, 60% of our country's forest areas are located in areas that are very sensitive to fire (Republic of Turkey Climate Change Action Plan 2011–2023, 2012; OGM, 2011; Ülgen et al., 2020). In addition, it is expected that the increase in air temperatures in future climate scenarios will increase the risk of a forest fire. In other words, increases in the length and severity of the hot and dry period in Turkey may also trigger wildfires.

According to the data of the Republic of Turkey Ministry of Agriculture and Forestry, the total number of wildfires is 114,941 in 83 years from 1937 to the end of 2020. It has been recorded that a total of 1 million 711,973 hectares of land were burned in these fires in Turkey. This value is approximately 15 hectares per fire. However, it is observed that both the number of fires and the amount of burned area per fire have decreased towards the present day. As follows, a total of 90, 956 hectares of lands were burned in 26, 311 wildfires between 2011 and 2020. According to these records, the average burned area per fire has been 3.5 hectares in the last 10 years.

However, wildfires, which were seen in a large part of Turkey in August 2021, causing damage to much larger areas, especially the rest of Muğla and Antalya Regional Directorates, reached the level of disaster with the effect of meteorological features. The wildfire started on 28 July 2021 in Manavgat, Antalya, and was brought under the control on 12 August 2021. In the "firestorm" that took place in many large and small areas between 28 July and 12 August, 8 people died, thousands of hectares of the forest area were burned, and many settlements were damaged. This "firestorm" ended on August 12, 2021, with the extinguishing of the fire in the Köyceğiz, Muğla. However, forest fires between 28 July and 12 August 2021 were recorded as wildfires with the highest loss of area in the history of forest fires in Turkey.

Within the scope of this study, we aimed to examine the atmospheric conditions in the period when the fires were effective. The heatwave and the wind characteristics that increase the intensity of the hot air and the area of influence of the fire were evaluated in Muğla and Antalya provinces on 25 July and 15 August 2021. A total of 24688 hectares of forest area, the size of 34563 football fields, was burned in 35 wildfires that broke out within the boundaries of Muğla Regional Directorate during the examination dates. In the same period, a total of 304 hectares of forest area, the size of 425 football fields, was burned in 41 forest fires that broke out within the borders of Antalya regional directorate.

Data And Method

In the scope of the study, the temperature and wind data of 63 meteorological stations were used in Antalya and Muğla provinces (Figure 1). Buishand's, Von Neumann's, and Pettitt homogeneity tests were applied for the daily temperatures of the stations with long-term data. In general, there is a significant increasing trend in the temperatures when the homogeneity noticeably deteriorates. The homogeneity of station temperatures has changed inhomogeneity after the 1990s (Table 1).

In another part of the study, we focused on the evaluation of atmospheric conditions in wildfire areas in 2021. For this purpose, we evaluated hourly temperature, wind direction, and speed, Isparta rawinsonde observations and meteorological maps (location, 700, 800, 500, hPa) between 25 July and 15 August 2021.

Table 1

homogeneity tests result of the stations with long-term data for the months of June, July and August (Dark color indicates statistical significance).

Haziran	Pettitt's test			Buishand's test			von Neumann's test	
İstasyonlar	*K*	*t*	*p-value*	*Q*	*t*	*p-value*	*N*	*p-value*
Bodrum	**1146**	1994	< 0.0001	**23.67**	1994	< 0.0001	**1.16**	< 0.0001
Muğla	**1208**	1989	< 0.0001	**22.56**	1989	< 0.0001	**1.49**	0.007
Dalaman	**614**	1992	0.000	**16.77**	1992	0.000	**1.19**	0.000
Fethiye	**827**	1994	0.000	**17.01**	1994	0.001	**1.36**	0.001
Datça	**688**	1992	< 0.0001	**19.92**	1992	< 0.0001	**0.80**	< 0.0001
Marmaris	352	1996	0.055	9.74	1996	0.050	**1.10**	0.000
Antalya	**1106**	1976	< 0.0001	**21.32**	1976	< 0.0001	**1.40**	0.002
Alanya	**994**	1992	< 0.0001	**24.74**	1992	< 0.0001	**0.65**	< 0.0001
Finike	**566**	1994	< 0.0001	**15.40**	1995	0.000	**1.22**	0.001
Kaş	42	2009	0.367	3.02	2009	0.751	1.92	0.421
Milas	**554**	1996	< 0.0001	**16.44**	1997	< 0.0001	**0.96**	< 0.0001
Yatağan	**561**	1993	< 0.0001	**17.73**	1994	< 0.0001	**1.10**	0.000
Köyceğiz	**550**	1996	< 0.0001	**15.59**	1996	0.000	**0.99**	< 0.0001
Korkuteli	**488**	1994	< 0.0001	**14.92**	1994	0.000	**1.18**	0.001
Elmalı	**586**	1994	< 0.0001	**16.43**	1994	0.000	**1.36**	0.004
Manavgat	**494**	1996	0.001	**15.33**	1996	0.000	**1.48**	0.025

Ağustos	Pettitt's test			Buishand's test			von Neumann's test	
İstasyonlar	*K*	*t*	*p-value*	*Q*	*t*	*p-value*	*N*	*p-value*
Bodrum	**1142**	1997	< 0.0001	**23.25**	1997	< 0.0001	**1.00**	< 0.0001
Muğla	**1227**	1984	< 0.0001	**22.07**	1997	< 0.0001	**1.17**	< 0.0001
Dalaman	**638**	1997	0.000	**16.67**	1997	< 0.0001	**1.31**	0.002
Fethiye	**740**	1997	0.002	**15.99**	1997	0.001	**1.24**	0.000
Datça	**717**	1991	< 0.0001	**21.31**	1991	< 0.0001	**0.76**	< 0.0001
Marmaris	**425**	2001	0.008	**10.84**	1967	0.021	**0.79**	< 0.0001
Antalya	**994**	1979	0.001	**18.84**	1979	0.000	**1.59**	0.025
Alanya	**892**	1992	< 0.0001	**22.18**	1992	< 0.0001	**0.71**	< 0.0001
Finike	**582**	1989	< 0.0001	**16.21**	1989	0.000	**1.55**	0.040
Kaş	**111**	2009	0.025	**7.17**	2009	0.011	1.61	0.149
Milas	**490**	2001	0.001	**12.13**	2001	0.005	**0.89**	< 0.0001
Yatağan	**622**	1997	< 0.0001	**19.49**	1997	< 0.0001	**0.89**	< 0.0001
Köyceğiz	**569**	2001	< 0.0001	**11.66**	2001	0.002	**0.82**	< 0.0001
Korkuteli	**606**	1997	< 0.0001	**18.60**	1997	< 0.0001	**1.08**	0.000
Elmalı	**514**	1998	0.003	**14.52**	1998	0.001	**1.37**	0.005
Manavgat	**401**	2001	0.017	10.39	2001	0.028	**0.97**	< 0.0001

Temmuz	Pettitt's test			Buishand's test			von Neumann's test	
İstasyonlar	*K*	*t*	*p-value*	*Q*	*t*	*p-value*	*N*	*p-value*
Bodrum	**1190**	1994	< 0.0001	**24.25**	1994	< 0.0001	**0.84**	< 0.0001
Muğla	**1476**	1985	< 0.0001	**27.12**	1985	< 0.0001	**0.94**	< 0.0001
Dalaman	**608**	1996	< 0.0001	**15.79**	1996	0.000	**1.40**	0.008
Fethiye	**789**	1999	0.001	**16.76**	1996	0.001	**1.07**	< 0.0001
Datça	**647**	1992	< 0.0001	**19.36**	1992	< 0.0001	**0.82**	< 0.0001
Marmaris	272	1999	0.299	8.85	1967	0.097	**1.06**	< 0.0001
Antalya	**971**	1976	0.001	**18.88**	1976	0.000	**1.45**	0.003
Alanya	**950**	1994	< 0.0001	**23.61**	1994	< 0.0001	**0.66**	< 0.0001
Finike	**498**	1994	0.001	**14.05**	1994	0.001	**1.03**	< 0.0001
Kaş	63	1999	0.751	4.42	1999	0.328	1.59	0.149
Milas	**496**	2001	0.000	**15.41**	2001	0.000	**0.82**	< 0.0001
Yatağan	**640**	1995	< 0.0001	**20.06**	1995	< 0.0001	**0.70**	< 0.0001
Köyceğiz	**560**	1999	< 0.0001	**16.01**	1999	< 0.0001	**0.75**	< 0.0001
Korkuteli	**604**	1995	< 0.0001	**18.92**	1995	< 0.0001	**0.86**	< 0.0001
Elmalı	**670**	1996	< 0.0001	**18.02**	1996	< 0.0001	**1.12**	0.000
Manavgat	334	1998	0.085	9.49	2000	0.064	**1.26**	0.002

Conrad and Pollak (1950) stated in their study that homogeneity, which is one of the main conditions in climate-related scientific studies, can only be evaluated as homogeneous in the case of climate-related changes. Since the inhomogeneity of the temperature data used in the study is related to the increasing trends in the minimum and maximum temperatures, these stations were used in the analyzes in the study.

After the homogeneity tests, heatwaves were calculated in the long-term data of the stations. For this purpose, long-term daily temperature data and hourly temperature data for 2021 were used in the 63 meteorology stations. Antalya and Muğla provinces are the areas where summer temperatures are high in Turkey.

In heatwave studies, temperature data are usually ordered from largest to smallest, and evaluations are made by considering the distribution of the extreme data in the relevant seasons. Threshold values generally used in studies are 90% and 95% percentiles. The consecutive temperature data calculated according to threshold values is the second most basic condition of heatwaves. If the calculated high temperatures continue uninterruptedly for 5-6 days (90th percentile) or 3 days (95th percentile) according to the determined threshold values, depending on the effective atmosphere circulation, the temperatures increase for a long time or for a shorter time.

The heatwave index used in the study was determined as the days where the maximum temperature in the hot season is at the 95th percentile and above, for 3 consecutive days and above (Xu. et al., 2013; Tong et al., 2010; Basagaña et al., 2011). In the study, the threshold used for the heatwave is the 95th percentile. In addition, in order for the high temperature to be considered a heatwave, it is required to experience these high temperatures for at least 3 consecutive days. Only 14 of the stations used in this context have long-term temperature data, while the data at some of the other stations are approximately 10-15 years. The short duration data of the stations were used to ensure homogeneity in the spatial evaluation of the heatwave.

In the last part of the study, forest fire areas were evaluated in Antalya and Muğla provinces. It is intended to provide a standard for the display of forest fire observations. This data set is provided by NASA Near Real-Time VNP14IMGTDL_NRT VIIRS 375 m Active Fire Detections. Therefore, data on forest fire areas in Turkey were obtained from (Schroeder et. al., 2014).

Results

When the distribution of the fires that took place is examined according to the causes, 47% of the fires were neglected, 32% were due to unknown reasons, 11% were natural and 10% were intentional 1997-2020 in Turkey (OGM, 2020). Negligence, vandalism, and fires of unknown origin are the causes of fire with the greatest spatial losses (Figure 2).

One of the most important reasons triggering the development of fires is the atmospheric conditions and topographic features of the area. Forest areas often become vulnerable to fire due to atmospheric conditions. Especially during heatwaves, more areas can be affected by the fire. In addition, wind conditions have a great effect on increasing fragility depending on the topography. Foehn winds can strengthen the development of fire by causing increased sensitivity in forest areas.

In recent years, Mediterranean Basin has experienced increases in extreme temperatures and heatwaves (Stefanon et al., 2012; Erlat et al., 2021; Kuglitsch et al., 2010). Forest areas in the Mediterranean Basin

have sensitivity and vulnerability to variations in atmospheric conditions.

Within the scope of the study, the temporal changes of the heatwaves were evaluated in the past years. In addition, heatwaves and atmospheric conditions were explained at the time of the wildfires in 2021. For this purpose, the surface and the upper atmosphere data were used in the study.

Temporal Distributions of Heatwaves

An increasing trend is observed in the year-to-year distribution of heatwaves. This increasing trend is similar to the increase in the summer night and day temperatures in Turkey and the Mediterranean basin. Especially since 1995, there has been a significant increase in the number of heatwaves in these areas. The 2007-2008 years were the most heatwaves in Turkey. The highest number of heatwaves in both provinces was experienced between 1998, 2007, 2008, and 2010. The maximum temperatures experienced during this period are above 39-40°C in many stations (Figure 3a).

Heatwaves are most experienced in July and August. In the south of Turkey, Antalya and Muğla experience at least 2 heatwaves each year. Their duration is between 3-4 days in some years and 5-7 days in some years. The similarity of the changes in the heat waves from year to year in these two areas displays that they developed under the influence of the same atmospheric circulation. However, due to the spatial variability of topographic features in Muğla, it is seen that heatwaves do not cause long-term high temperatures at every station (Figure 3b). Total heatwave events are experienced more in Antalya than in Muğla and these heatwaves cause higher temperatures in Antalya (Figure 3c).

Heatwave in July - August 2021

The maximum temperatures in Antalya and Muğla provinces were calculated to be above the 95th percentile as of July 26-27. Also, in most of the stations, these high temperatures are consecutive for 3 days or more. The high-temperature days were recorded before the start of the fires in the southern part of Turkey. One of the most important factors increasing the effect size of the fire disaster is the heatwave experienced synchronically (Figure 4).

The heatwave was experienced in all the stations around the southern part of Turkey, before the forest fire that started in Manavgat on July 28. As of 28 July, high surface air temperatures affected the initial conditions of the fire, and the fires, which broke out due to negligence, unknown, and vandalism, spread rapidly in the regions. In addition, it is enunciable that the circulation of the upper atmosphere in the fire areas has a great effect on the inadequacy of the forest fire interventions.

As of July 28, the development of a ridge from northern Africa to the Balkans and western Turkey is evident. In the area where the ridge is effective, high-pressure conditions are effective on the surface (Figure 5a). Subsidence air tends to heat adiabatically. A similar process continued in August and similar circulation conditions were effective in both the surface and upper atmosphere in the same region. At these levels, temperatures are also approximately -5 ℃. The hot air, which penetrated towards the south of Europe, the Eastern Mediterranean, and Anatolia over Africa and the Arabian Peninsula, continued to

strengthen its effect from time to time in mid-August (Figure 5b). Skew-T Log P diagram of Isparta rawinsonde station was used to evaluate the synoptic conditions in the forest fire areas. Isparta station is at 37.75° N latitude, 30.55° E longitude, and 997 meters elevation. According to the 00:00 observation on 28.07.2021, inversion developed at 705-700 hPa (3106-3178 m). The 705 hPa level (3106 m) is the condensation level of the station. At this level, the water vapor in the atmosphere condenses into a water droplet. However, the fact that the condensation level is so high can be explained by the low amount of moisture in the atmosphere. The wind speed is approximately 30 knots (55.56 km/h) at 700 hPa. Inversion was effective at 890-880 hPa (1095-1194 m) of Isparta station on 02.08.2021. The condensation level on rising air is approximately 679 hPa (3400 m). At this time, the activity of hot air masses that are weak in terms of moisture content, due to the effect of hot air intruding into the south of Europe and Anatolia through northern Africa and the Arabian Peninsula. Inversions at lower levels caused large-scale fire smoke to remain in the lower atmosphere in early August (Fig. 7a&b).

According to the distribution of wind directions and speeds of 300hPa, the westerly winds continue to flow eastward as the Hadley cell in the north of Algeria in the west of the Mediterranean basin. Winds blowing from the north of Libya to the northeast in the middle of the basin made a small wave from the west of Turkey and continued its flow towards the Caspian Sea. The speed of the wind, which is effective at 300hPa, is between 1.6 and 31.6 m/sec. The wind speed is approximately 30 m/sec over Turkey (Figure 8a).

According to Gönençgil (1993a), the foehn wind is not only a wind consisting of local conditions but should be in a medium-scale atmospheric circulation that is affected by orographic conditions and anticyclonic conditions of the upper atmosphere together. In Figures 5a and b, upper atmospheric conditions that fit this description have evolved appropriately. In particular, the circulation conditions mentioned in the Gönençgil (1990 and 1993b) studies show a significant improvement at wind flows of 700 hPa.

The pressure gradient between the effect of the monsoon circulation towards the Persian Gulf and the high-pressure center on the Black Sea caused the wind speeds to strengthen in places over Turkey. The flow directions of surface winds are mostly of nature to carry the character of the direction in which they blow (Figure 8b).

The speed of the northern sector wind, which is effective in the areas where the forest fires spread widely between 28 July and 12 August, is generally between 5-8 m/sec. This wind sometimes played a role in making fire interventions difficult in areas where it was effective at approximately 18-29 km/h (Figure 8c).

According to Gönençgil (1993a and 1993b) studies, the fact that winds stay above 10 m/sec is the first factor that prepares the blow-dry conditions. In addition, as mentioned in the same studies, when a cyclone enters the field through the Mediterranean Sea or Basra, the blow dryer character gains speed. On such days in Antalya and its surroundings, the prevailing wind directions in the ground and upper atmosphere are northern sectors.

It is also possible to see the strengthening gradient effect as etesian winds on the west coast of Turkey. In addition, the flows heading towards the Mediterranean Sea through Anatolia exceed the Taurus mountains and cause foehn winds in the areas of the Mediterranean coastal belt.

Etesian winds partially weaken the effect of the heatwave in Western Anatolia. In the Mediterranean coastal zone, especially around Antalya and Muğla, the blow-dry effect causes the hot air effect to intensify.

Spatial Distribution of Wildfires and Wind Characteristics of the Area

The fires in 2021 can be considered as one of the fires that cause the most significant losses in Turkey. The fires started at different points simultaneously in the Manavgat district of Antalya on July 28. Fire areas are visualized according to the start dates of fires. The fires started simultaneously at many different points on the same day (Figure 9a). The reasons for the exit of the fires around Manavgat are indicated as unknown (unknown), unidentified (unidentified fire-raising) according to the data of the General Directorate of Forestry. The first starting points of the fires lasted until August 12, including large forest areas around it (Figure 9b). Around Antalya, the fires that lasted for the first two weeks of August, neglect, and carelessness at many points, and accidents (electrical lines) were experienced. Fires in Muğla started on 29 July. Fires that started on the Bozburun Peninsula and on the mountainside of Gölgeli (Figure 9c) In August, in addition to these areas, fires broke out in the forest scrub in the north of Gökova Bay (Figure 9d). The fires that lasted for a long time were concentrated in certain areas as visualized in the relevant maps in Figure 9. The fact that the fires could not be brought under control until mid-August caused the ecosystem in this area to be completely lost.

The wind direction and speed information of the meteorology stations in the fire area between 28 July and 12 August are shown in Figure 7 together with the topographic characteristics of the area. The speed, direction, and frequency of the wind are the most important parameters that affect the climatological characteristics of the environment during the heatwave period. The local wind conditions have increased the effects of the heatwave. According to the wind roses, the stations are generally under the influence of the northerly circulation during the fire period.

The fact that the daily maximum wind speeds are above 10 m/sec is a factor that prepares the Foehn. For example, on July 29, when the forest fires continued, the speed of the northerly wind was 8.2 m/sec in Antalya and 12.1 m/sec at Antalya Akseki station (Figure 10).

Between 28 July and 5 August 2021, 21 forest fires were experienced in Antalya province and 14 forest fires were experienced in Muğla. The fires in the region lasted until August 12, 2021. Between 28 July and 12 August, 425 football fields (304 hectares) and 34563 football fields (24688 hectares) were burned in Antalya and Muğla, respectively. During the fire period, the heatwave and the increase in the speed of the wind (foehn wind) have made it difficult to fight at fire sites. At the same time, these areas have also made them vulnerable to forest fires caused by negligence, unknown, and vandalism.

Conclusion And Discussion

Forest fires occurred in many parts of Turkey for different reasons between 28 July and 12 August 2021. Most of the fires took place in the provinces of Antalya and Muğla. Within the scope of the study, atmospheric conditions were evaluated during the fires caused by negligence, unknown, and vandalism. For this reason, it was focused on the areas of responsibility of Muğla and Antalya Regional Directorates of Forestry. In this context, temperature and wind data of 63 meteorology stations and upper atmosphere observations were examined and evaluated.

Homogeneity tests were applied for the temperature data of the stations in the study area in the past periods. The temperature variability/trends of the stations were evaluated from the recording period to the present. The inhomogeneity of the temperatures was due to the change in the 1990s. After the 1990s, the inhomogeneity of temperatures is strongly related to the increasing warming trends.

In addition, hourly temperature, pressure, wind direction, and speed data as well as meteorological maps (surface, 700 hPa, 800 hPa, and 500 hPa) were evaluated within the scope of the study between 25 July and 15 August 2021. The upper atmospheric flow was mapped during the forest fire period. Heatwaves at the stations were calculated in the long-term period.

According to an assessment by the authorities of Turkey, 34563 sizes of football fields were burned in forest areas within the borders of Mugla Regional Directorate. In the same period, a forest area the size of 425 football fields was burned within the borders of Antalya regional directorate.

One of the most important factors causing the development of wildfires and the disruption of the intervention is the heatwave experienced in Antalya and Muğla provinces. At the time of the forest fire, the region is generally dominated by warm air masses. According to the data from Isparta rawinsonde station, the lack of moisture in the air masses at the time of the start of fires caused an increase in the influence of the fire. At the same time, the northernly airflow was flowing through Turkey towards the Basra low pressure. This northerly airflow caused a foehn wind around Muğla and Antalya. The heatwave and strong foehn wind caused increased sensitivity to fire in this area. Atmospheric conditions during the fires caused severe loss of forest areas and biodiversity in these areas.

Declarations

Acknowledge

We acknowledge the use of imagery from the NASA Near Real-Time VNP14IMGTDL_NRT VIIRS 375 m Active Fire Detections.

Author contributions ZA: conceptualization, methodology, data analysis, writing the original draft. BG: supervision, conceptualization, methodology, review and editing. OH: review.

Funding: The authors did not receive support from any organization for the submitted work. No funding was received to assist with the preparation of this manuscript.

Conflict of interest The authors declare that they have no known competing financial interests or personal relationships that could have appeared to influence the work reported in this paper.

Data availability Statement

The data are available upon request to zacar@comu.edu.tr

References

1. A. V. Zayats, I. I. Smolyaninov, and A. A. Maradudin (2005) Nano-optics of surface plasmon polaritons. Physics reports 408, 131-314.
2. J. Zhang, L. Zhang, and W. Xu (2012) Surface plasmon polaritons: physics and applications. Journal of Physics D: Applied Physics 45, 113001.
3. B. Wang, X. Zhang, X. Yuan, and J. Teng (2012) Optical coupling of surface plasmons between graphene sheets. Applied Physics Letters 100, 131111.
4. C. Qin, B. Wang, H. Huang, H. Long, K. Wang, and P. Lu (2014) Low-loss plasmonic supermodes in graphene multilayers. Optics Express 22, 25324-25332.
5. M. Jablan, H. Buljan, and M. Soljačić (2009) Plasmonics in graphene at infrared frequencies. Physical review B 80, 245435.
6. Z. Liu, X. Zhang, Z. Zhang, E. Gao, F. Zhou, H. Li, and X. Luo (2020) Simultaneous switching at multiple frequencies and triple plasmon-induced transparency in multilayer patterned graphene-based terahertz metamaterial. New Journal of Physics 22, 083006.
7. X. Zhang, Z. Liu, Z. Zhang, E. Gao, X. Luo, F. Zhou, H. Li, and Z. Yi (2020) Polarization-sensitive triple plasmon-induced transparency with synchronous and asynchronous switching based on monolayer graphene metamaterials. Optics Express 28, 36771-36783.
8. A. Fardoost, F. G. Vanani, A. a. Amirhosseini, and R. Safian (2016) Design of a multilayer graphene-based ultrawideband terahertz absorber. IEEE Transactions on Nanotechnology 16, 68-74.
9. Y. Cai, J. Zhu, and Q. H. Liu (2015) Tunable enhanced optical absorption of graphene using plasmonic perfect absorbers. Applied Physics Letters 106, 043105.
10. Y. Wang, Y. Yi, D. Xu, Z. Yi, Z. Li, X. Chen, H. Jile, J. Zhang, L. Zeng, and G. Li (2021) Terahertz tunable three band narrowband perfect absorber based on Dirac semimetal. Physica E: Low-dimensional Systems and Nanostructures 131, 114750.
11. Y. Zhao, and Y. Zhu (2015) Graphene-based hybrid films for plasmonic sensing. Nanoscale 7, 14561-14576.
12. Xia S X, Zhai X, Wang L L, et al (2020) Polarization-independent plasmonic absorption in stacked anisotropic 2D material nanostructures. Optics Letters, 45(1): 93-96.

13. G. Xu, J. Sun, H. Mao, and T. Pan (2018) Surface plasmon-enhanced near-field thermal rectification in graphene-based structures. Journal of Applied Physics 124, 183104.
14. Z. Zhang, Z. Liu, F. Zhou, J. Wang, Y. Wang, X. Zhang, Y. Qin, S. Zhuo, X. Luo, and E. Gao (2021) Broadband plasmon-induced transparency modulator in the terahertz band based on multilayer graphene metamaterials. JOSA A 38, 784-789.
15. X. Zhang, Z. Liu, Z. Zhang, Y. Qin, S. Zhuo, X. Luo, F. Zhou, Z. Yi, J. Wang, and Y. Wang (2021) Triple plasmon-induced transparency in graphene and metal metamaterials and its anomalous property. Journal of Physics D: Applied Physics 54, 284001.
16. Z. Liu, Z. Zhang, F. Zhou, X. Zhang, E. Gao, and X. Luo (2021) Dynamically tunable electro-optic switch and multimode filter based on twisted bilayer graphene strips. Journal of Optics 23, 025104.
17. C. Xiong, H. Xu, M. Zhao, B. Zhang, C. Liu, B. Zeng, K. Wu, B. Ruan, M. Li, and H. Li (2021) Triple plasmon-induced transparency and outstanding slow-light in quasi-continuous monolayer graphene structure. Science China Physics, Mechanics & Astronomy 64, 1-11.
18. Z. Liu, X. Zhang, F. Zhou, X. Luo, Z. Zhang, Y. Qin, S. Zhuo, E. Gao, H. Li, and Z. Yi (2021) Triple plasmon-induced transparency and optical switch desensitized to polarized light based on a mono-layer metamaterial. Optics Express 29, 13949-13959.
19. E. Gao, Z. Liu, H. Li, H. Xu, Z. Zhang, X. Luo, C. Xiong, C. Liu, B. Zhang, and F. Zhou (2019) Dynamically tunable dual plasmon-induced transparency and absorption based on a single-layer patterned graphene metamaterial, Optics express 27, 13884-13894.
20. Z. Chen, H. Chen, H. Jile, D. Xu, Z. Yi, Y. Lei, X. Chen, Z. Zhou, S. Cai, and G. Li (2021) Multi-band multi-tunable perfect plasmon absorber based on L-shaped and double-elliptical graphene stacks. Diamond and Related Materials 115, 108374.
21. H. Xu, M. Zhao, M. Zheng, C. Xiong, B. Zhang, Y. Peng, and H. Li (2018) Dual plasmon-induced transparency and slow light effect in monolayer graphene structure with rectangular defects. Journal of Physics D: Applied Physics 52, 025104.
22. Zheng Z, Zheng Y, Luo Y, et al. (2022) A switchable terahertz device combining ultra-wideband absorption and ultra-wideband complete reflection. Physical Chemistry Chemical Physics,.
23. X. Zhang, F. Zhou, Z. Liu, Z. Zhang, Y. Qin, S. Zhuo, X. Luo, E. Gao, and H. Li (2021) Quadruple plasmon-induced transparency of polarization desensitization caused by the Boltzmann function. Optics Express 29, 29387-29401.
24. H. Lu, Y. Li, H. Jiao, Z. Li, D. Mao, and J. Zhao (2019) Induced reflection in Tamm plasmon systems. Optics Express 27, 5383-5392.
25. H. Tian, Y. Yang, J. Tang, L. Jiang, and Y. Xiang (2021) Graphene Tamm plasmon-induced enhanced and tunable photonic spin hall effect of reflected light in terahertz band. Results in Physics 25, 104300.
26. Y. Yang, J. Li, J. Li, J. Huang, Y. Zhang, L. Liang, and J. Yao (2020) Plasmon-induced reflection metasurface with dual-mode modulation for multi-functional THz devices. Optics and Lasers in Engineering 127, 105969.

27. C. Liu, H. Li, H. Xu, M. Zhao, C. Xiong, M. Li, B. Ruan, B. Zhang, and K. Wu (2020) Dynamically tunable excellent absorber based on plasmon-induced absorption in black phosphorus nanoribbon. Journal of Applied Physics 127, 163301.
28. Y. Neo, T. Matsumoto, T. Watanabe, M. Tomita, and H. Mimura (2016) Transformation from plasmon-induced transparence to-induced absorption through the control of coupling strength in metal-insulator-metal structure. Optics Express 24, 26201-26208.
29. Y. Qin, F. Zhou, Z. Liu, X. Zhang, S. Zhuo, X. Luo, C. Ji, G. Yang, Z. Zhou, and L. Sun (2022) Triple plasmon-induced transparency and dynamically tunable electro-optics switch based on a multilayer patterned graphene metamaterial. JOSA A 39, 377-382.
30. S. Zhuo, F. Zhou, Y. Liu, Z. Liu, X. Zhang, X. Luo, Y. Qin, G. Yang, C. Ji, and Z. Zhou (2022) Terahertz multimode modulator based on tunable triple-plasmon-induced transparency in monolayer graphene metamaterials. JOSA A 39, 594-599.
31. Z. Liu, E. Gao, Z. Zhang, H. Li, H. Xu, X. Zhang, X. Luo, and F. Zhou (2020) Dual-mode on-to-off modulation of plasmon-induced transparency and coupling effect in patterned graphene-based terahertz metasurface. Nanoscale research letters 15, 1-9.
32. Zhang X, Liu Z, Zhang Z, et al. (2021) Polarization-sensitive triple plasmon-induced transparency with synchronous and asynchronous switching based on monolayer graphene metamaterials. Optics Express, 28(24): 36771-36783.
33. C. Liu, H. Li, H. Xu, M. Zhao, C. Xiong, M. Li, B. Ruan, B. Zhang, and K. Wu (2020) Plasmonic biosensor based on excellently absorbable adjustable plasmon-induced transparency in black phosphorus and graphene metamaterials. New Journal of Physics 22, 073049.

Figures

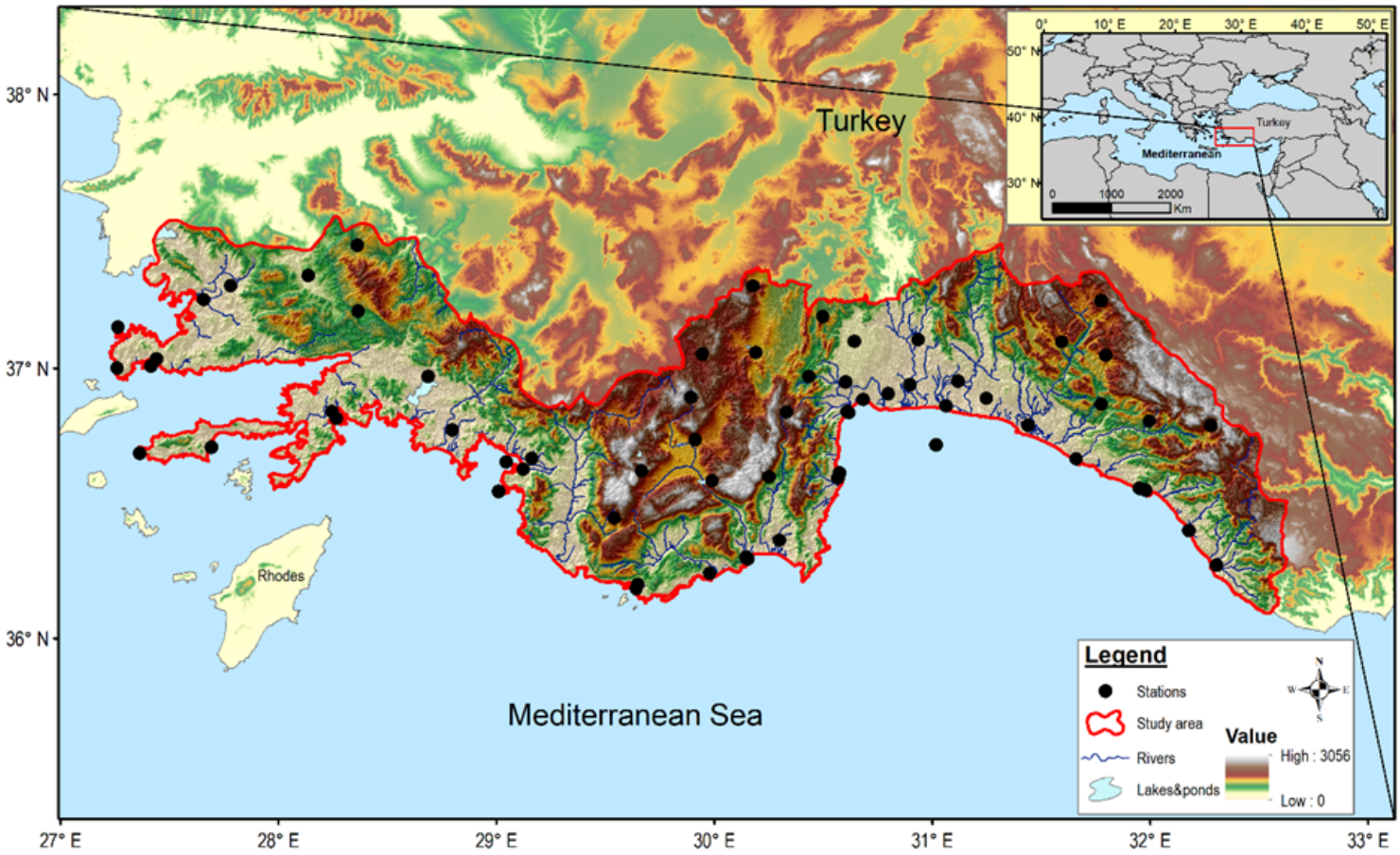

Figure 1

Geographical distribution of the stations used in the study and the location of the study area.

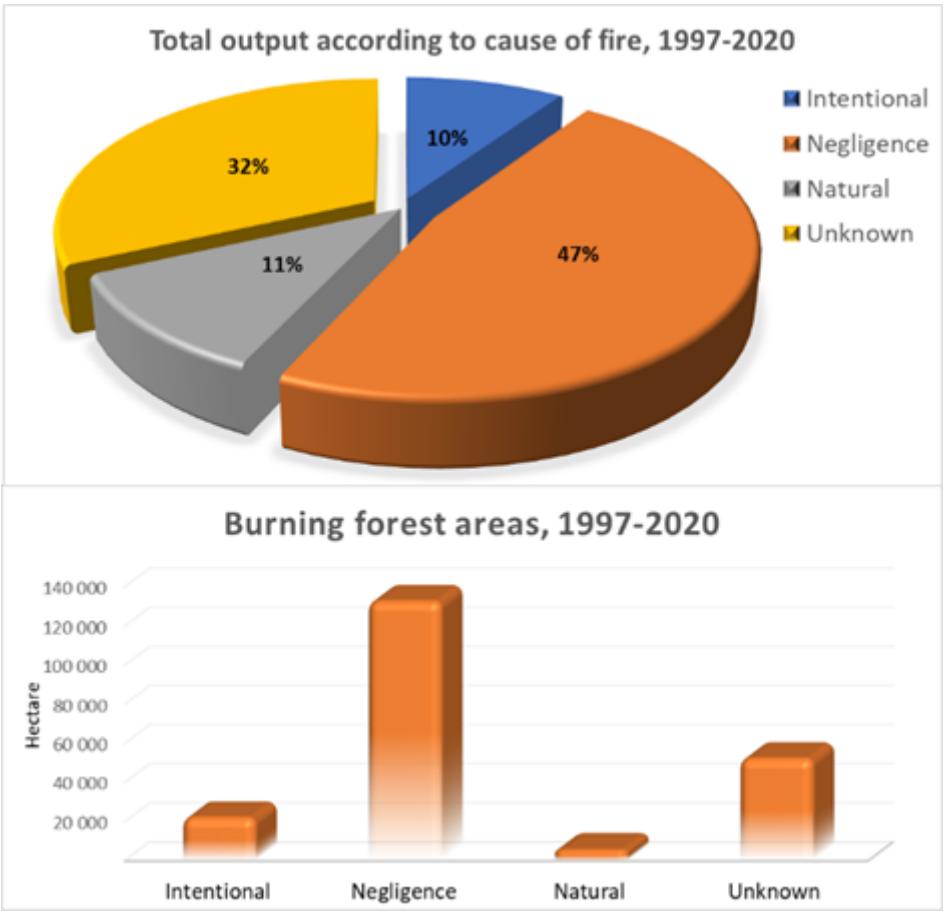

Figure 2

Total output according to cause of fire and burning forest area in 1997-2020

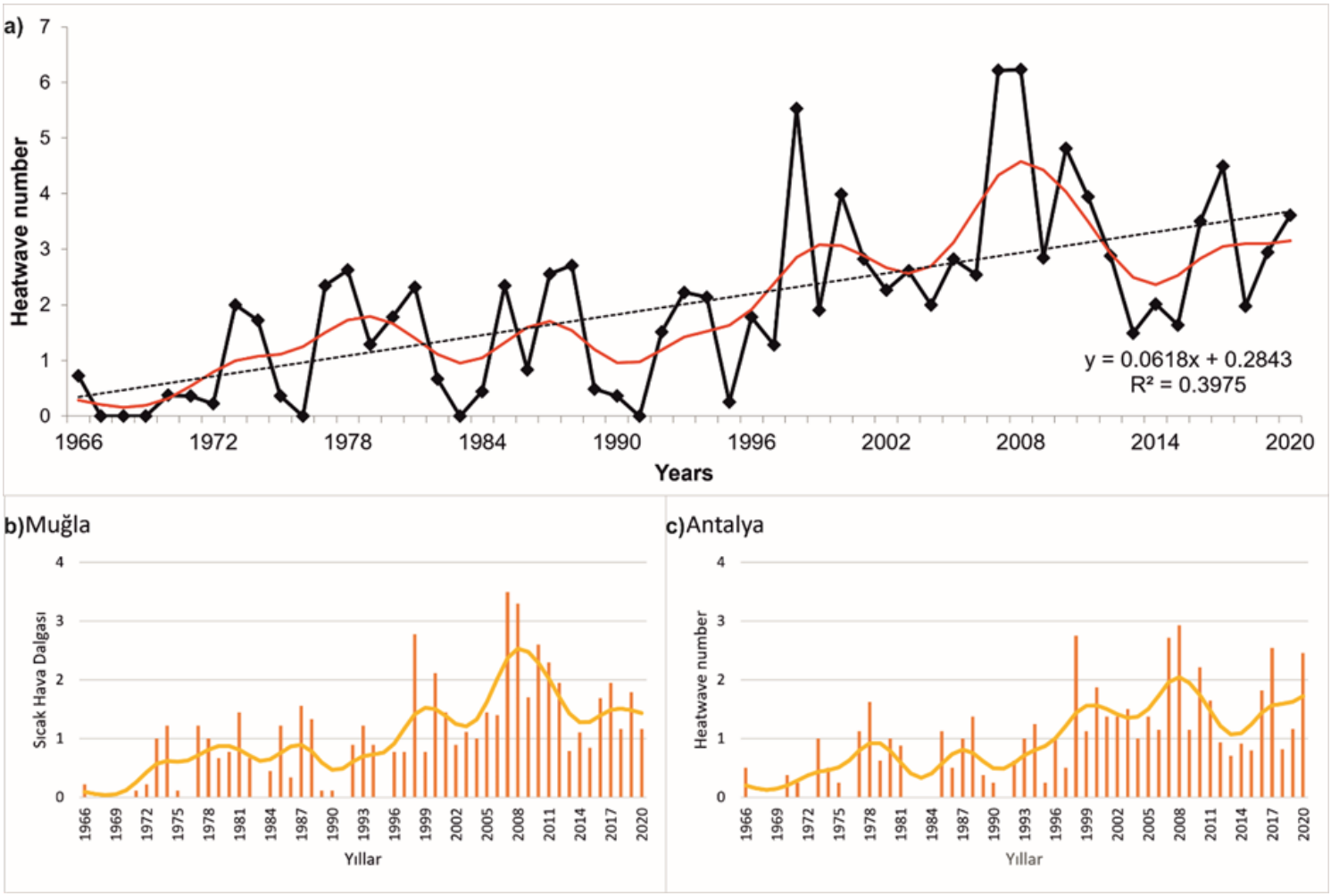

Figure 3

Distribution of heatwaves in Muğla and Antalya provinces by years.

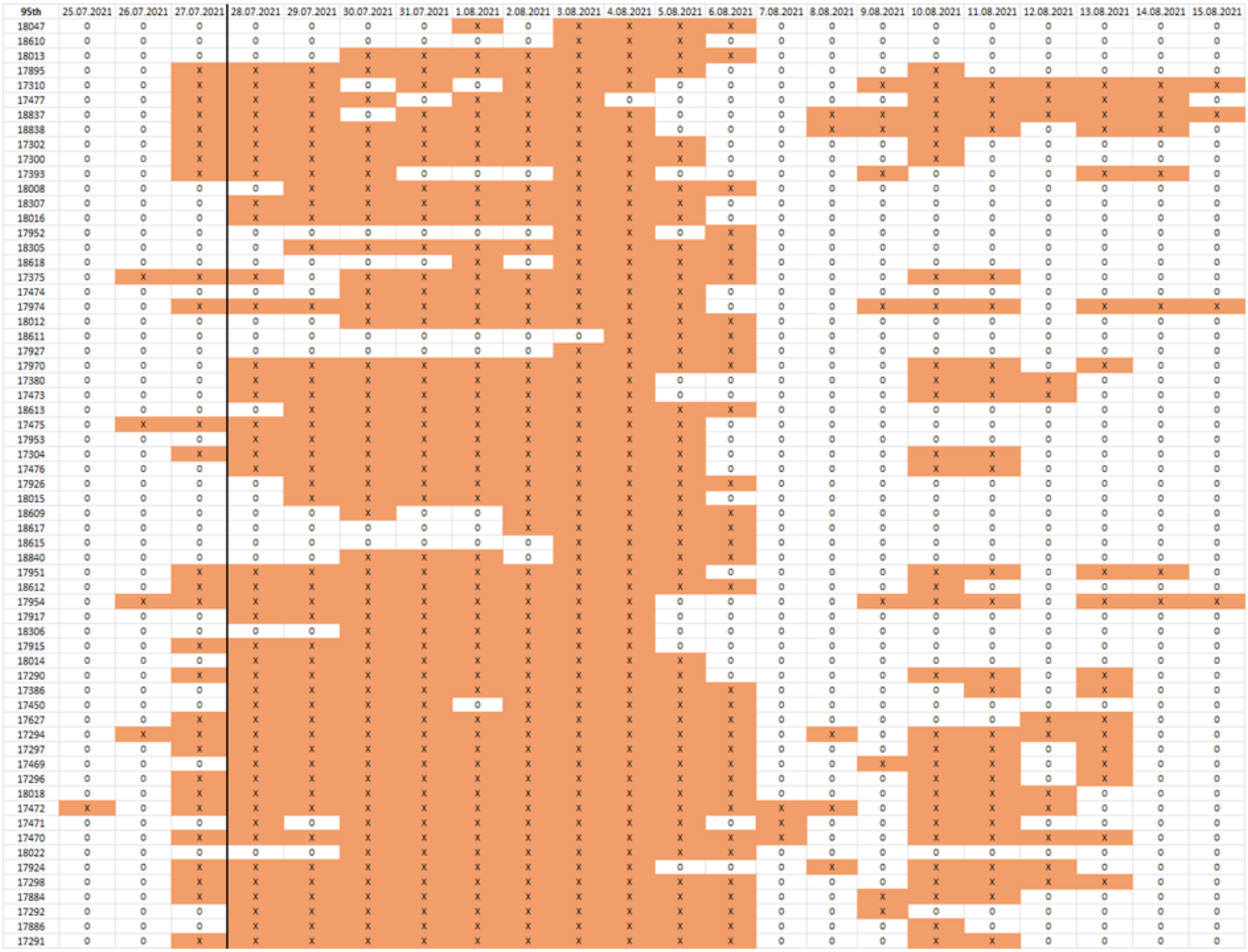

95th	25.07.2021	26.07.2021	27.07.2021	28.07.2021	29.07.2021	30.07.2021	31.07.2021	1.08.2021	2.08.2021	3.08.2021	4.08.2021	5.08.2021	6.08.2021	7.08.2021	8.08.2021	9.08.2021	10.08.2021	11.08.2021	12.08.2021	13.08.2021	14.08.2021	15.08.2021
18047	0	0	0	0	0	0	0	X	0	X	X	X	X	0	0	0	0	0	0	0	0	0
18610	0	0	0	0	0	0	0	0	0	X	X	X	0	0	0	0	0	0	0	0	0	0
18013	0	0	0	0	0	X	X	X	X	X	X	X	X	0	0	0	0	0	0	0	0	0
17895	0	0	X	X	X	X	X	X	X	X	X	X	0	0	0	0	X	0	0	0	0	0
17310	0	0	X	X	X	0	X	0	X	X	X	0	0	0	0	X	X	X	X	X	X	X
17477	0	0	X	X	X	X	0	X	X	X	0	0	0	0	0	0	X	X	X	X	X	0
18837	0	0	X	X	X	0	X	X	X	X	X	0	0	0	X	X	X	X	X	X	X	X
18838	0	0	X	X	X	X	X	X	X	X	X	0	0	0	X	X	X	X	0	X	X	0
17302	0	0	X	X	X	X	X	X	X	X	X	X	0	0	0	0	X	0	0	0	0	0
17300	0	0	X	X	X	X	X	X	X	X	X	X	0	0	0	0	X	0	0	0	0	0
17393	0	0	X	X	X	X	0	0	0	X	X	0	0	0	0	X	0	0	0	X	X	0
18008	0	0	0	0	X	X	X	X	X	X	X	X	X	0	0	0	0	0	0	0	0	0
18307	0	0	0	X	X	X	X	X	X	X	X	X	0	0	0	0	0	0	0	0	0	0
18016	0	0	0	X	X	X	X	X	X	X	X	X	0	0	0	0	0	0	0	0	0	0
17952	0	0	0	0	0	0	0	0	0	X	X	0	X	0	0	0	0	0	0	0	0	0
18305	0	0	0	0	X	X	X	X	X	X	X	X	X	0	0	0	0	0	0	0	0	0
18618	0	0	0	0	0	0	0	X	0	X	X	X	X	0	0	0	0	0	0	0	0	0
17375	0	X	X	X	0	X	X	X	X	X	X	X	X	0	0	0	X	X	0	0	0	0
17474	0	0	0	0	0	X	X	X	X	X	X	X	0	0	0	0	0	0	0	0	0	0
17974	0	0	X	X	X	X	X	X	X	X	X	X	0	0	0	X	X	X	0	X	X	X
18012	0	0	0	0	0	X	X	X	X	X	X	X	X	0	0	0	0	0	0	0	0	0
18611	0	0	0	0	0	0	0	0	0	0	X	X	X	0	0	0	0	0	0	0	0	0
17927	0	0	0	0	0	0	0	0	0	X	X	X	X	0	0	0	0	0	0	0	0	0
17970	0	0	0	X	X	X	X	X	X	X	X	X	X	0	0	0	X	X	0	X	0	0
17380	0	0	0	X	X	X	X	X	X	X	X	0	0	0	0	0	X	X	X	0	0	0
17473	0	0	0	X	X	X	X	X	X	X	X	0	0	0	0	0	X	X	X	0	0	0
18613	0	0	0	0	X	X	X	X	X	X	X	X	X	0	0	0	0	0	0	0	0	0
17475	0	X	X	X	X	X	X	X	X	X	X	X	0	0	0	0	0	0	0	0	0	0
17953	0	0	0	X	X	X	X	X	X	X	X	X	0	0	0	0	0	0	0	0	0	0
17304	0	0	X	X	X	X	X	X	X	X	X	X	0	0	0	0	X	X	0	0	0	0
17476	0	0	0	X	X	X	X	X	X	X	X	X	0	0	0	0	X	X	0	0	0	0
17926	0	0	0	0	X	X	X	X	X	X	X	X	X	0	0	0	0	0	0	0	0	0
18015	0	0	0	0	X	X	X	X	X	X	X	X	0	0	0	0	0	0	0	0	0	0
18609	0	0	0	0	0	X	0	0	X	X	X	X	X	0	0	0	0	0	0	0	0	0
18617	0	0	0	0	0	0	0	0	X	X	X	X	X	0	0	0	0	0	0	0	0	0
18615	0	0	0	0	0	0	0	0	0	X	X	X	X	0	0	0	0	0	0	0	0	0
18840	0	0	0	0	0	X	X	X	0	X	X	X	X	0	0	0	0	0	0	0	0	0
17951	0	0	X	X	X	X	X	X	X	X	X	X	0	0	0	0	X	X	0	X	X	0
18612	0	0	X	X	X	X	X	X	X	X	X	X	X	0	0	0	X	0	0	0	0	0
17954	0	X	X	X	X	X	X	X	X	X	X	0	0	0	0	X	X	X	0	X	X	X
17917	0	0	0	X	X	X	X	X	X	X	X	0	0	0	0	0	0	0	0	0	0	0
18306	0	0	0	0	0	X	X	X	X	X	X	0	0	0	0	0	0	0	0	0	0	0
17915	0	0	X	X	X	X	X	X	X	X	X	0	0	0	0	0	0	0	0	0	0	0
18014	0	0	0	X	X	X	X	X	X	X	X	X	0	0	0	0	0	0	0	0	0	0
17290	0	0	X	X	X	X	X	X	X	X	X	X	0	0	0	0	X	X	0	X	0	0
17386	0	0	0	X	X	X	X	X	X	X	X	X	X	0	0	0	0	X	0	X	0	0
17450	0	0	0	X	X	X	X	0	X	X	X	X	X	0	0	0	0	0	0	0	0	0
17627	0	0	X	X	X	X	X	X	X	X	X	X	X	0	0	0	0	0	X	X	0	0
17294	0	X	X	X	X	X	X	X	X	X	X	X	X	0	X	0	X	X	X	X	0	0
17297	0	0	X	X	X	X	X	X	X	X	X	X	X	0	0	0	X	X	0	X	0	0
17469	0	0	0	X	X	X	X	X	X	X	X	X	X	0	0	X	X	X	0	X	0	0
17296	0	0	X	X	X	X	X	X	X	X	X	X	X	0	0	0	X	X	0	X	0	0
18018	0	0	X	X	X	X	X	X	X	X	X	X	X	0	0	0	X	X	X	0	0	0
17472	X	0	X	X	X	X	X	X	X	X	X	X	X	X	X	0	X	X	X	0	0	0
17471	0	0	0	X	0	X	X	X	X	X	X	X	0	X	0	0	X	X	0	0	0	0
17470	0	0	X	X	X	X	X	X	X	X	X	X	X	X	0	0	X	X	X	X	0	0
18022	0	0	0	0	0	X	X	X	X	X	X	X	X	0	0	0	0	0	0	0	0	0
17924	0	0	X	X	X	X	X	X	X	X	X	0	0	0	X	0	X	X	X	0	0	0
17298	0	0	X	X	X	X	X	X	X	X	X	X	X	0	0	0	X	X	X	X	0	0
17884	0	0	X	X	X	X	X	X	X	X	X	X	X	0	0	X	X	X	0	0	0	0
17292	0	0	0	X	X	X	X	X	X	X	X	X	X	0	0	X	0	0	0	0	0	0
17886	0	0	0	X	X	X	X	X	X	X	X	X	X	0	0	0	X	0	0	0	0	0
17291	0	0	X	X	X	X	X	X	X	X	X	X	X	0	0	0	X	X	0	0	0	0

Figure 4

The distribution of the maximum temperatures above the 95th percentile in the stations on 25 July and 15 August 2021 (The black line is the date of the fire that started in Manavgat).

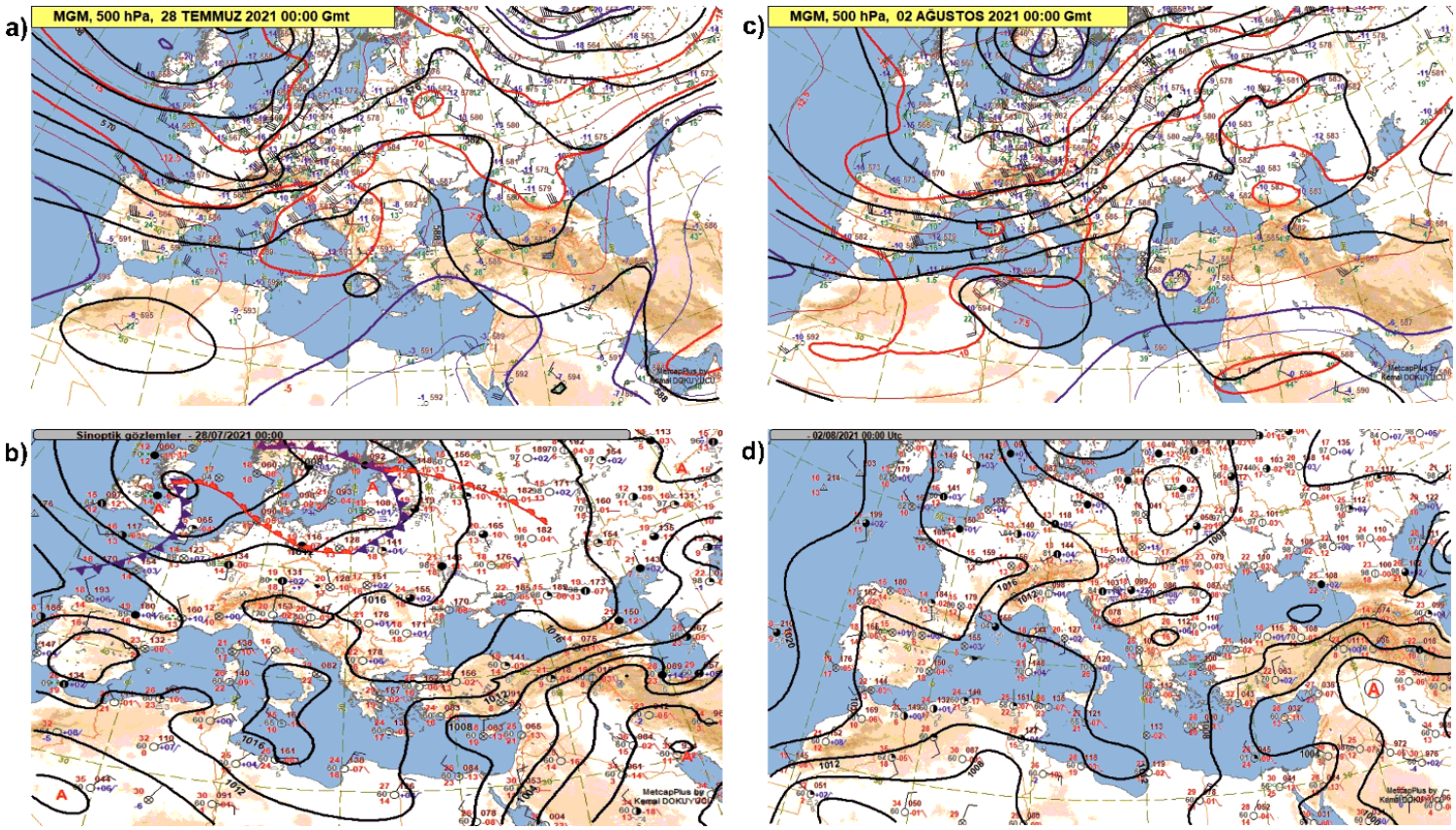

Figure 5

Contour and isotherm at 00:00 GMT surface and 500 hPa level as a) 28.07.2021 & b) 02.08.2021.

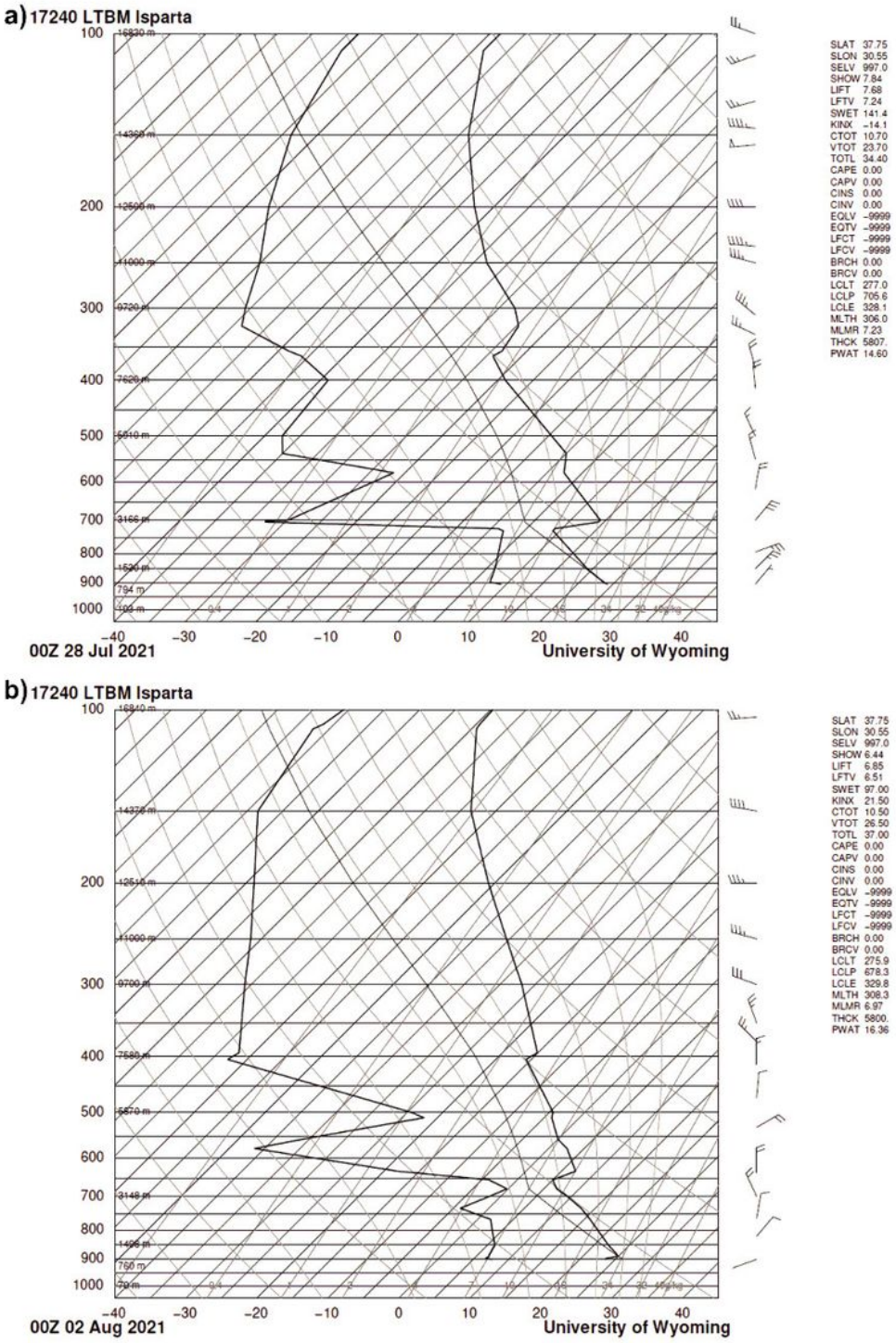

Figure 6

Skew-T Log P diagrams of Isparta rawinsonde station on a) 28.07.2021 and b) 02.08.2021.

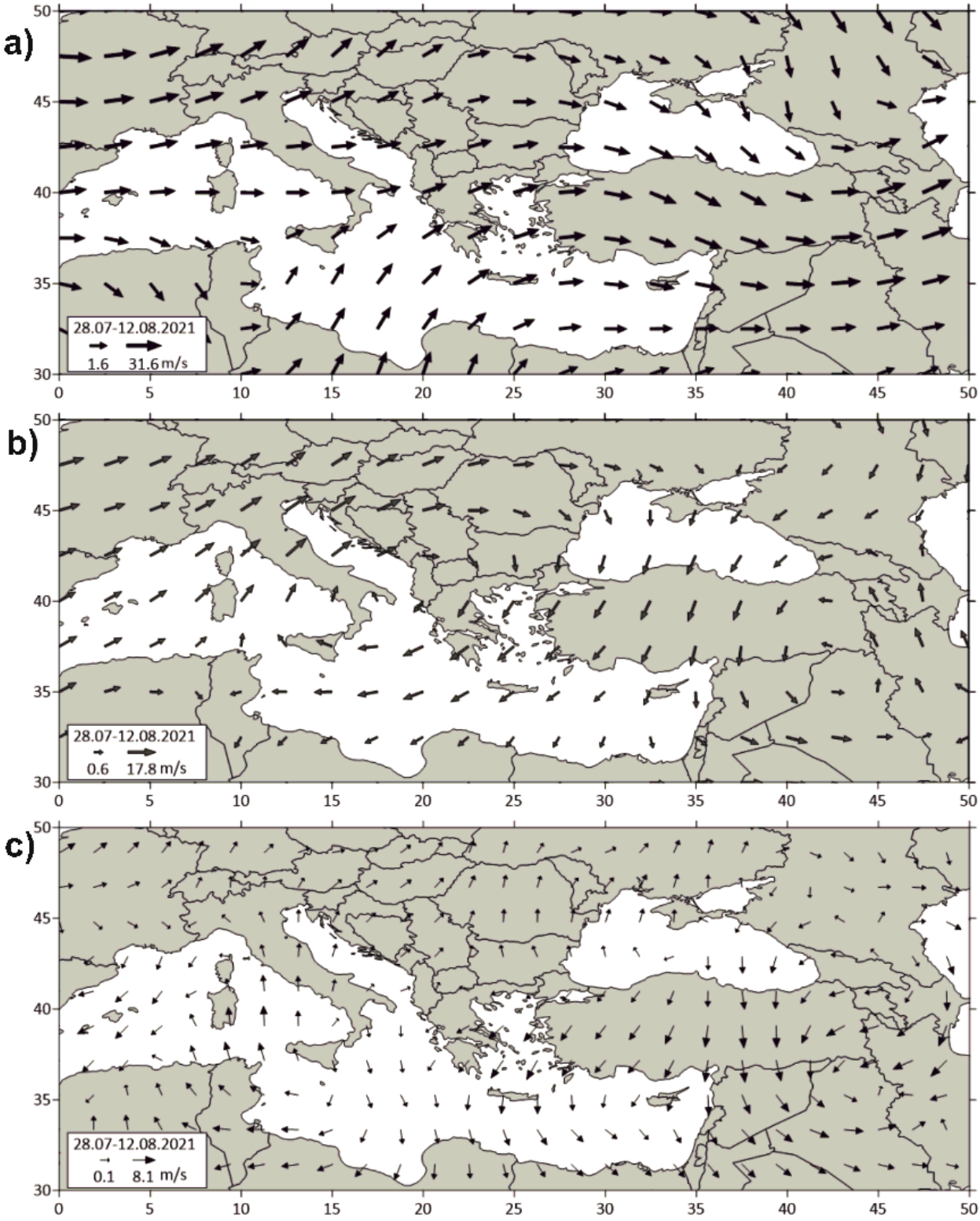

Figure 7

Wind directions and speeds at a)300hPa and b)700hPa c) 10m levels between on 28 July and 12 August 2021.

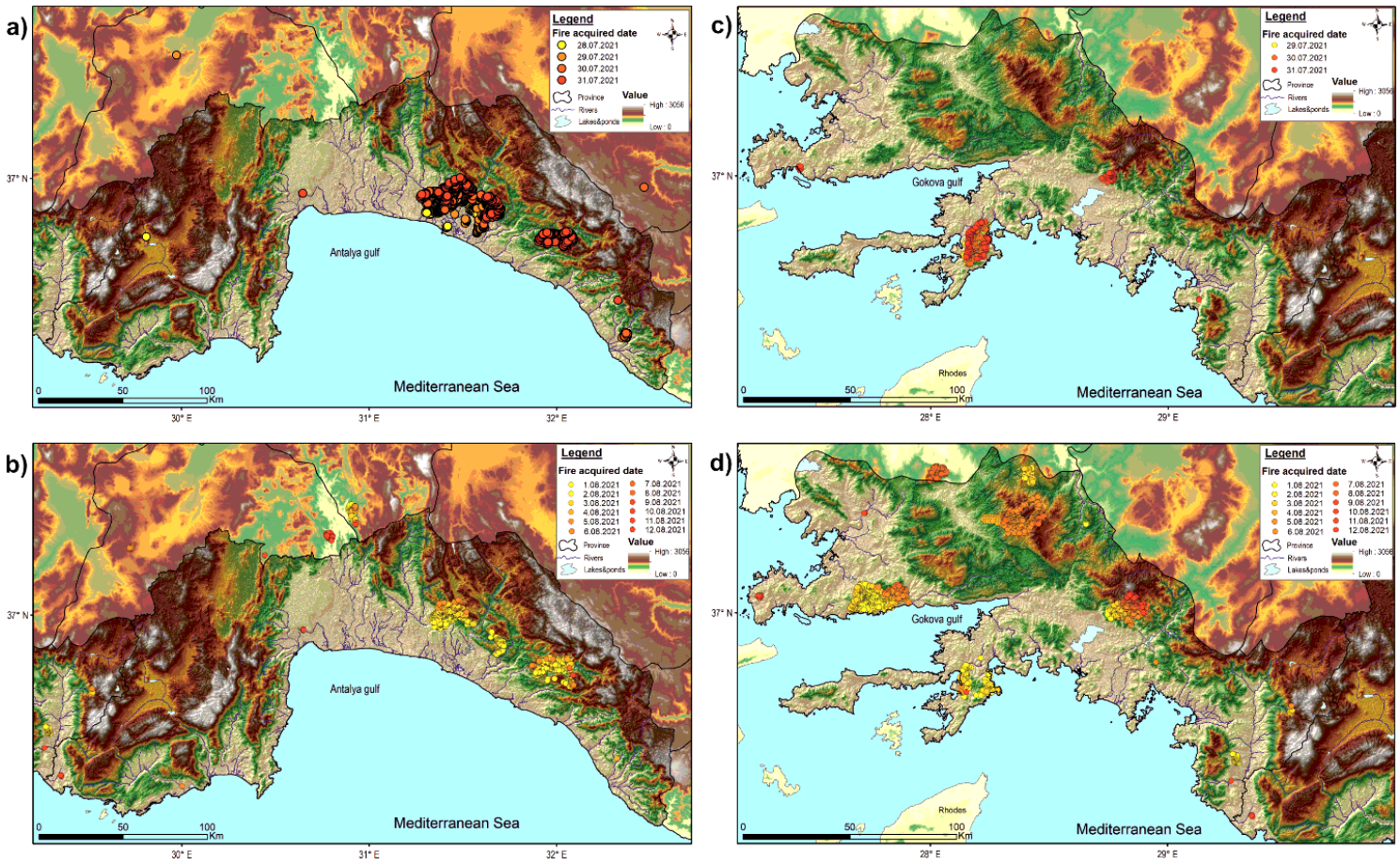

Figure 8

Geographical distribution of fires by fire acquired date **a)** Antalya Province in July, **b)** Antalya Province in August, **c)** Mugla Province in July, **d)** Mugla Province in August.

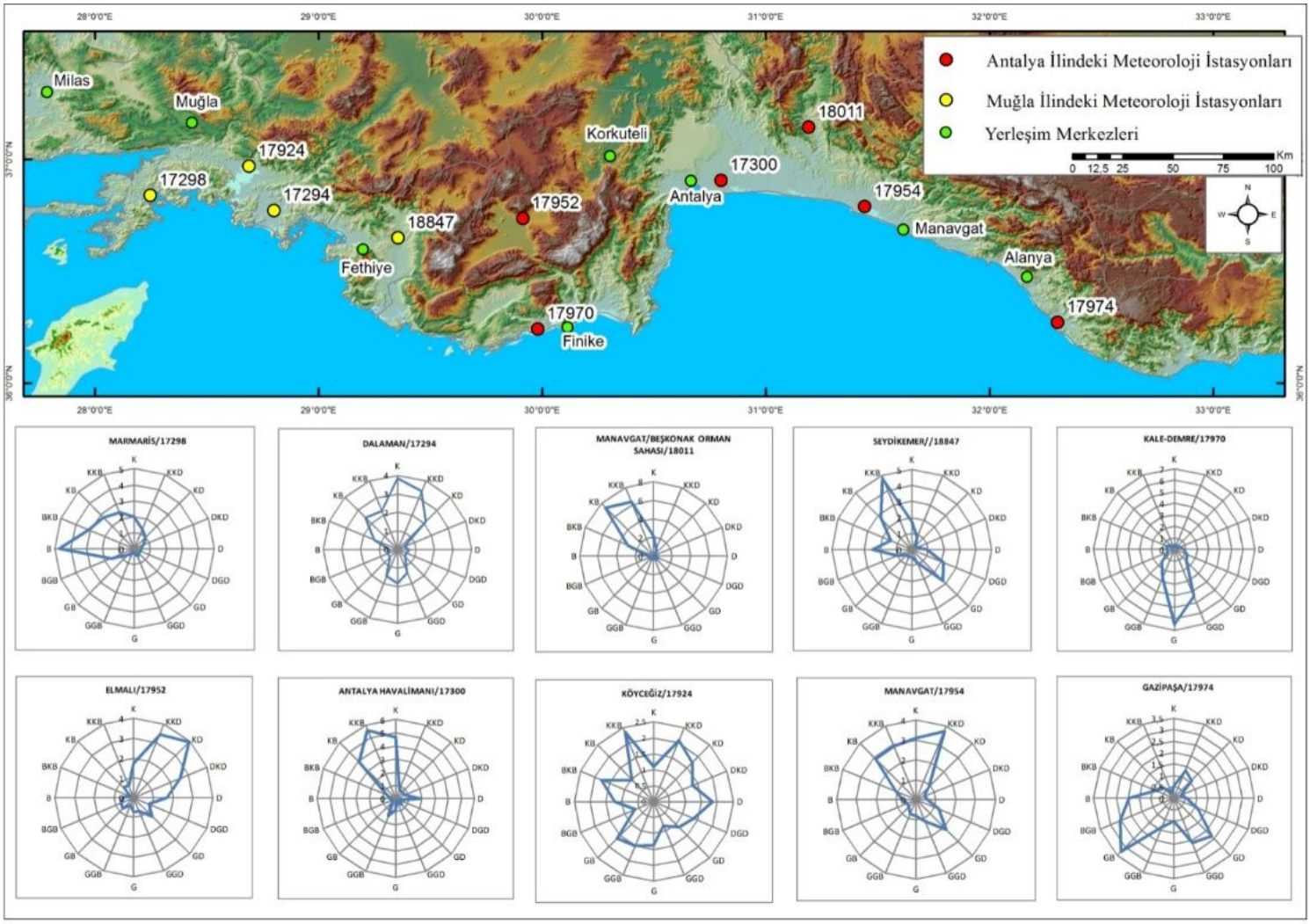

Figure 9

Wind roses of the stations in the study area during the fire period.